Title

ANALYSIS OF INTERFERENCE DATA IN A HIGHLY HETEROGENEOUS NATURALLY FRACTURED GEOTHERMAL RESERVOIR

Authors

Benson, S.M.
Lai, C.H.

Publication Date

1984-09-01

Lawrence Berkeley Laboratory
UNIVERSITY OF CALIFORNIA

EARTH SCIENCES DIVISION

Presented at the 59th Annual Technical Conference
and Exhibition of the Society of Engineers of AIME,
Houston, TX, September 16-19, 1984

ANALYSIS OF INTERFERENCE DATA IN A HIGHLY HETEROGENEOUS NATURALLY FRACTURED GEOTHERMAL RESERVOIR

S.M. Benson and C.H. Lai

September 1984

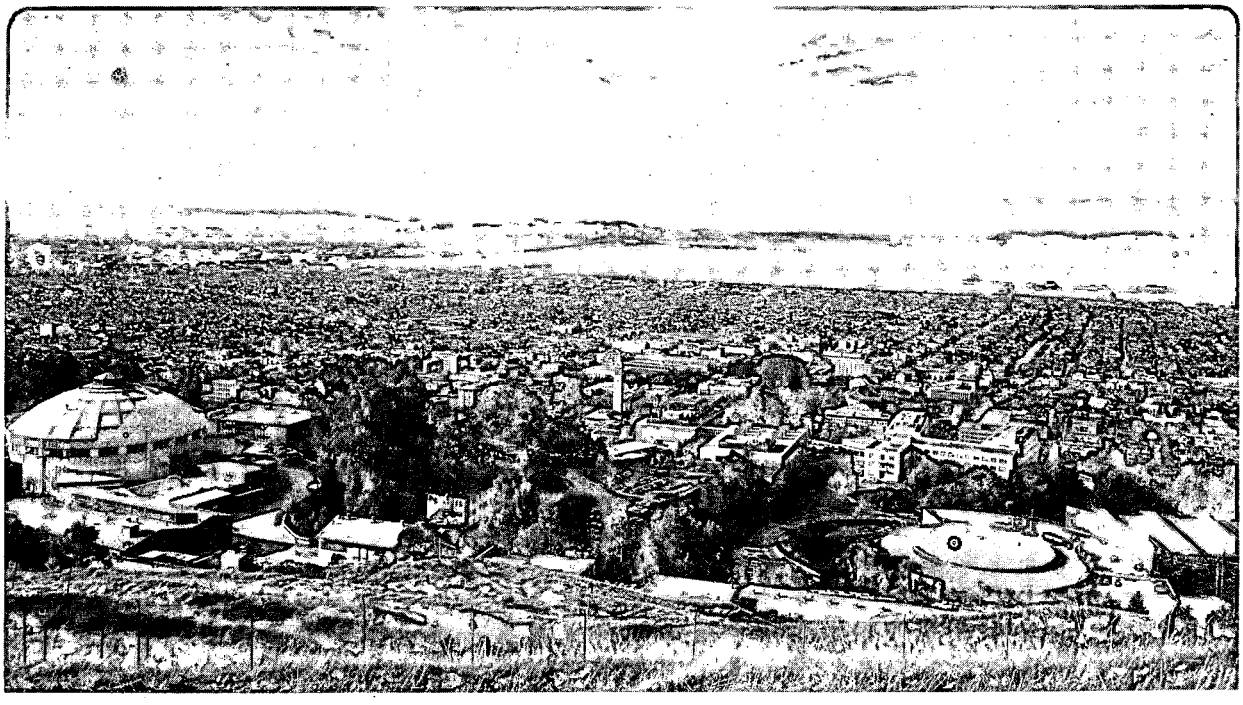

Prepared for the U.S. Department of Energy under Contract DE-AC03-76SF00098

DISCLAIMER

Presented at the 59th Annual Technical Conference and Exhibition of the Society of Engineers of AIME held in Houston, Texas, September 16-19, 1984.

LBL-17450

ANALYSIS OF INTEREFERENCE DATA IN A HIGHLY HETEROGENEOUS NATURALLY FRACTURED GEOTHERMAL RESERVOIR

Sally M. Benson and C. H. Lai

Earth Sciences Division
Lawrence Berkeley Laboratory
University of California
Berkeley, California 94720

September 1985

This work was supported by the Assistant Secretary of Conservation and Renewable Energy, Office of Renewable Technology, Division of Geothermal and Hydropower Technologies of the U.S. Department of Energy under Contract DE-AC03-76SF00098.

ANALYSIS OF INTERFERENCE DATA IN A HIGHLY HETEROGENEOUS NATURALLY FRACTURED GEOTHERMAL RESERVOIR

by S.M. Benson and C.H. Lai, Lawrence Berkeley Laboratory

This paper was presented at the 59th Annual Technical Conference and Exhibition held in Houston, Texas, September 16–19, 1984. The material is subject to correction by the author. Permission to copy is restricted to an abstract of not more than 300 words. Write SPE, 6200 North Central Expressway, Drawer 64706, Dallas, Texas 75206 USA. Telex 730989 SPEDAL.

ABSTRACT

Data from an eleven-well interference test in a highly heterogeneous naturally fractured reservoir are analyzed. The data show excellent agreement with the theoretical results for double-porosity reservoirs. Using both type-curve and semi-logarithmic techniques, the permeability-thickness, storativity, and double-porosity parameters (λ and ω) are determined. Both methods of analysis yield the same values for these parameters. However, a combination of both techniques results in greater confidence in the analysis. Systematic variations of the storativity, with increasing distance from the production well, are obtained from the interference data analysis. It is shown that this variation is the result of a high permeability region surrounding the pumped well and penetrated by several of the observation wells. A new graphical technique is developed for determining the size and permeability of this region.

INTRODUCTION

It has long been recognized that interference testing is a valuable tool for the evaluation of reservoir parameters. Pressure changes measured in a passive well in response to the pumping of a nearby well can be interpreted to yield values for permeability-thickness (kh) and storativity (ϕch), as well as indicate the presence and location of reservoir heterogeneities (e.g., boundaries,[1] anisotropy,[2] fluid banks,[3] layering,[4] double-porosity,[5] etc.). However, since the solutions may be highly non-unique, accurate interpretation of the data requires an adequate geologic model of the system in order to determine the appropriate mathematical solution.[6] This paper describes the interpretation of an eleven-well interference test in the Klamath Falls, Oregon, geothermal reservoir. The complexity of the geologic system precludes the development of a hydrogeologic model based solely on lithologic data.[7,8] However, by combining the results of hydrologic tests with geologic data, a convincing hydrogeological model of the system is developed.

References and illustrations at end of paper.

BACKGROUND

The geothermal resource at Klamath Falls has been used for more than 50 years to heat homes and to provide hot water for both domestic use and a variety of small scale industrial applications.[9] The geothermal anomaly and its geologic setting have been the subject of numerous research efforts.[7,8,10,11] The results relevant to the present work are summarized below.

Geologic Setting

The Klamath Falls geothermal anomaly is a shallow (< 2000 ft deep), moderate-temperature (100°C) system. The geothermal reservoir occurs in rocks of primarily volcanic origin, including both andesitic flows and volcanic sediments. Over 450 wells have been drilled into the reservoir. Well lithologies show that massive basaltic and andesitic units are interbedded with tuff, volcanic sediments, diatomites, and thin lava flows. In spite of the wealth of data from the resource, the extent and geologic characteristics of the reservoir are still ill-defined because correlation of lithologic units is often impossible, even over distances as short as 100 ft.[8] The area is also transected by a major NW-trending normal fault that is presumably the primary conduit along which thermal fluids rise from great depths to the surface.[7,8]

No single rock type or structural feature can be identified as the source of the system's permeability. Drilling data show that the contacts between layers, fractured basalts, lavas, and tuff units are often highly permeable. For example, a spinner survey (not shown) from the well shown in Figure 1 indicates that two permeable layers intersect the well, each accounting for approximately 50% of the total permeability-thickness. The first layer occurs at a depth of 470 to 520 ft, in a shale and tuff unit (or at the contacts above and below it), and the second at a depth of 1020 to 1080 ft, in the middle of a thick unit of basalt interbedded with shale.[12] The spacing between permeable formations varies from well to well; some wells have several per hundred feet and some have one per thousand feet.

The normal fault that transects the area probably creates highly permeable vertical conduits.

Previous Testing

Several short (less than 1 day) interference tests have been conducted in the Klamath Falls geothermal reservoir.[13,14,15] Interpretations of these tests have shown that the reservoir is highly permeable[13] and that the pressure transients are characteristic of a double-porosity reservoir.[16] The short duration of these tests prevented conclusive evaluation of the reservoir parameters and their spacial variations.

INTERFERENCE TEST DESCRIPTION

The interference test, which covered a seven-week period in July-August, 1983, consisted of measuring pressure changes in nine wells while pumping and injection operations were ongoing in two other wells. For the first three weeks, well CW-1 was pumped at a rate of 24,700 bbl/D (43.5 kg/s). For the final four weeks, water was pumped from CW-1 and concurrently reinjected into the County Museum well. Back-pressure at the injection well resulted in a slightly lower and somewhat variable pumping rate (23,800 to 22,600 bbl/D). Figure 2 shows the pumping and reinjection schedule. The figure also shows the downhole pressure response at one of the observation wells. During the first phase of the test the pressure dropped (approximately 1.7 psi in this well). After reinjection began, the pressure gradually increased to within 0.4 psi of the original value. This response is typical of each of the nine observation wells shown in Figure 3.[8]

Well Descriptions

An area of approximately 1 square mile was monitored during the interference test. Observation, pumping (CW-1) and injection (County Museum) well locations are shown in Figure 3. Table 1 lists the depths, casing-top elevations, open intervals, and distances to the active wells for each well used during the test. Well depths range from 250 ft to over 1200 ft. However, each well penetrates at least part of the same reservoir (as is evident from the test and drilling data). Wells in this area are drilled until at least one, and usually two permeable units are encountered. Typically, wells are completed with all of the permeable intervals open to the wellbore.

The injection well completion is shown in Figure 1. As mentioned previously, a spinner survey showed that 50% of the fluid is injected between 470 and 520 ft and the remaining 50% between 1020 and 1080 ft. The pumped well, although 900 ft deep, produces from a perforated interval between 195 and 240 ft.[8]

Instrumentation

The high permeabilities in this formation and correspondingly small drawdowns require that high-resolution instrumentation be used to measure pressure changes. Also, the high permeabilities result in rapid transmission of the pressure disturbance through the reservoir. Therefore, careful synchronization of the clocks against which measurements are made is important (pressure changes are apparent in nearby wells within 10 seconds after a rate change). For this test all observation well measurements were made with high resolution quartz crystal pressure transducers.[17] The data were transmitted to a central location where they were processed and recorded. Data were recorded every 10 seconds immediately following a pumping or injection rate change and every 10 minutes otherwise. The combination of highly accurate pressure measurements with synchronous data recording resulted in excellent quality data.

INTERFERENCE DATA ANALYSIS

The fractured, faulted, and heterogeneous nature of this system, interpretation of previous short term tests, and shape of the drawdown and buildup curves suggest that a double-porosity (or layered) model best describes the pressure transient responses in the observation wells.[8,16,18] Pressure transients in double-porosity systems are characterized by three periods; the first one is representative of the fracture system, the second of a transition period, and the last of the bulk system parameters.[5,19] The presence of these three regions in the actual data depends on the ratios of the permeabilities, porosities, compressibilities, and geometry of the system.[16,21,22] Interference data from such systems can be analyzed to determine kh and $\phi c h_t$.[5,21] If the double-porosity nature of the reservoir is reflected in the data, then the parameters λ and ω can be determined using one of several procedures described in the literature.[5,16,20,22,23] For this study, two methods of analysis are used, a log-log type-curve matching technique presented by Deruyck et al.[16], and a semi-log history-matching technique that uses a mathematical solution developed by Lai et al.[22] The parameters ω and λ are those defined by Warren and Root[19] as

$$\omega = \phi_f c_f / (\phi_f c_f + \phi_m c_m) \quad (1)$$

$$\lambda = \alpha r_w^2 (k_m / k_f) \quad (2)$$

Prior to a discussion of the results of the interference test analysis, two additional points should be mentioned. First, pressure transients due to the initial pumping phase of the test are ignored in the analysis of the injection test data. Second, the small flowrate variations (< 5%) during the injection phase of the test are neglected. The errors resulting from these approximations are minimized by considering only the first two weeks of data from the injection phase of the test.

Type Curve Analysis

Deruyck et al.[16] presented two sets of type-curves for analyzing pressure transient data in naturally fractured systems - one for pseudo-steady state flow between the fractures and the matrix and another for transient inter-porosity flow. Both sets of curves are applicable to the classical double-porosity reservoir described by Barenblatt et al.[24], as well as to layered

formations in which only the high permeability layers produce fluid into the wellbore. To analyze data with these type-curves, a log(Δp) versus log(Δt) plot is prepared. Values of λ and ω are determined from the curve for which the best-fit match is found. The parameters, kh and ϕch_t, are calculated from the match points by

$$kh = 141.2\ qB\mu\ (p_D/\Delta p) \quad (3)$$

$$\phi ch_t = 2.64 \times 10^{-4}\ (kh/\mu r^2)[\Delta t/(t_D/r_D^2)]/\omega \quad (4)$$

In this study, 13 pressure drawdowns and buildups are analyzed with these type-curves. Drawdown data from three of the observation wells are shown in Figures 4 through 6. These data are typical of the pressure transient responses in all of the wells during the pumping phase of the test. The data are matched to the type-curves for double-porosity reservoirs with transient inter-porosity flow. As shown by the type-curve matches in Figures 4 through 6, the agreement between the theoretical and actual data is excellent. For all observation wells, data from 30 seconds to over 400 hours can be matched to a single theoretical curve.[8] Also note that even though the largest drawdown is less than 2 psi; it is possible to measure the early-time data (drawdowns of less than 0.1 psi) necessary for accurate type-curve matching.

Values of the reservoir kh obtained from these three wells range from 1.4×10^6 to 1.7×10^6 md-ft. The agreement between the values is remarkably good, considering the complexity of the geologic system. On the other hand, ϕch_t, λ, and ω vary by over an order of magnitude. A discussion in the next section shows that the drawdown data are not very sensitive to variations in the double-porosity parameters and therefore, they may be insignificant. On the other hand, the differences in ϕch_t are significant and cannot be accounted for by a double-porosity model.

Pressure buildup curves in wells close to the injection well display typical double-porosity characteristics. The log-log data plots from two of the observation wells (Page, and Spires & Mest) are shown in Figures 7 and 8. Each shows the presence of three periods: i) an initial period when the pressure increases very rapidly (fracture response); ii) an intermediate period when the pressure reaches a plateau (matrix blocks supplying fluid to the fractures); and iii) a final period when the rate of pressure buildup increases to a new steady value (bulk system response).

For these wells, the pseudo-steady state model matches the data better than the transient inter-porosity flow model. This is demonstrated by the type-curve matches in Figures 7 and 8. The buildup data from the Page well, shown in Figure 7, gives an excellent match. The reservoir parameters obtained from this analysis (kh = 1.4×10^6 md-ft, $\phi ch_t = 7.3 \times 10^{-3}$ ft/psi, $\lambda = 2.4 \times 10^{-7}$ and $\omega = 0.06$) agree well with those obtained from the drawdown analyses. In Figure 8, two matches are shown for the Spires & Mest well data. The match shown by the solid line is for transient inter-porosity flow. It gives an excellent match to data from the first hour and last several hundred hours of the test. However, in the intermediate region, the predicted buildups are significantly greater than the actual values. For this match kh = 1.1×10^6 md-ft, $\phi ch = 8.3 \times 10^{-3}$ ft/psi, $\lambda = 8 \times 10^{-11}$, and $\omega = 6 \times 10^{-3}$. The low value of kh and the extremely low value of λ shed doubt on the validity of this interpretation. A second match of the data, this time to a pseudo-steady state curve (shown by the dashed line in Figure 8), gives an excellent match to all of the data after the first 6 minutes. Values of the reservoir parameters calculated from this match are closer to the average values. The poor match of the early-time data (< 6 minutes) is attributed to a local heterogeneity that is not accounted for by a double-porosity model. A conclusive explanation for why these data fit a pseudo-steady state inter-porosity model better than a transient flow model is not available at this time. One possible explanation is provided by Moench;[25] that is, flow from the matrix to the fractures is impaired by a fracture skin. Conceivably, precipitation of hydrothermal minerals on the fracture faces may reduce the surface permeability and lower the rate of flow into the fractures.[26]

Pressure buildup data from the Steamer well, located 2850 ft from the injection well, are shown in Figure 9. These data fit the Theis curve. Theoretical solutions indicate that double-porosity reservoirs appear to be homogeneous when observation wells are far from the active well. This is consistent with the Steamer well data.

Semi-log Analysis

To double-check the results of the type-curve analysis, the data were re-analyzed with a semi-logarithmic history-matching technique. To use this method, the pressure data are plotted versus log(Δt). The reservoir kh is calculated from the slope of the semi-log straight line drawn through the late time data points and ϕch_t from the time at which the semi-log straight line intersects the line where $\Delta p = 0$.[5,16,22] After kh and ϕch_t are determined, λ and ω are obtained by history-matching the data to theoretical drawdowns calculated for various combinations of these parameters. For this study, we use the mathematical solution presented by Lai et al., which accurately accounts for transient inter-porosity flow in a double-porosity reservoir with the block-like geometry originally proposed by Barenblatt et al.[24] and Warren and Root.[19]

The semi-log analyses of the drawdown data for three of the observation wells discussed previously are shown in Figures 10 through 13. As shown in each figure, the late-time data fall on a well-defined semi-log straight line. Calculated values of kh range from 1.5×10^6 to 1.9×10^6 md-ft. These values are in good agreement with the values obtained from the log-log analysis. A discussion of the well-by-well comparison of the parameters is reserved until the next section. Calculated values of ϕch_t range from 4.8×10^{-3} to 2.7×10^{-2} ft/psi. Again, the results are in good agreement with the log-log analyses and show that ϕch_t varys by an order of magnitude.

Figure 10 demonstrates the procedure for determining λ and ω. Drawdowns for numerous pairs of these parameters are calculated. The correct

values of λ and ω are then determined by the combination of these parameters that match the data best. Note however that large variations in λ and ω (over an order of magnitude) produce only slight changes in the shape of the drawdown curve. Thus, an erroneous match can be obtained easily. This aside, the curve for $\lambda = 6\text{x}10^{-7}$ and $\omega = 0.1$ appears to match the data best. These values agree reasonably well with the best ones obtained from the type-curve match ($\lambda = 1.9\text{x}10^{-7}$ and $\omega = 0.3$). Similar results are obtained from the data shown in Figures 11 and 12.

Discussion

In general, values of kh obtained from the drawdown and buildup analyses are remarkably consistent from well to well and between the two methods of analysis. Results of the individual well analysis, for both the type-curve and semi-log methods, are summarized in Table 2. Calculated permeabilities range from $1.1\text{x}10^{6}$ to $1.7\text{x}10^{6}$ md-ft for the type-curve analyses and from $1.0\text{x}10^{6}$ to $1.9\text{x}10^{6}$ md-ft for the semi-log analyses, showing that overall, the field behaves in a relatively uniform manner. A well-by-well comparison of the kh values obtained by the two analysis techniques shows that the values are usually within 10% of one another. However, for two analyses, they differ by as much as 30%. The type-curve technique gives more consistent results for kh (i.e., $kh_{max}/kh_{min} = 1.5$ for the type-curve analyses, in comparison to the ratio of 1.9 obtained from the semi-log analyses).

As mentioned previously, values of ϕch_t range over several orders of magnitude - from $1.1\text{x}10^{-3}$ to 0.79 ft/psi for the type-curve analyses and from $2.2\text{x}10^{-3}$ to 1.1 ft/psi for the semi-log analyses. With one exception, comparison of the values of ϕch_t calculated by the two methods show that they agree to within approximately 35% of each other. However, the anomalously high values and large variations in ϕch_t, calculated using both methods, cannot be explained by a double-porosity model. We propose that these variations are the result of a highly permeable region that surrounds the pumped well and is penetrated by the wells with anomalously high ϕch_t values. This proposal is discussed in detail in the following section.

Calculated values of λ and ω are also given in Table 2. Variations in these parameters are large; however, as was shown in the previous section, the drawdown curves are quite non-unique. Therefore, large variations in these parameters are not unexpected. Best estimates for λ and ω are 10^{-7} and 0.01, respectively.

COMPOSITE RESERVOIR ANALYSIS

A schematic of the system considered here is shown in Figure 13. There are two regions: an inner region with the properties k_1h, ϕ_1, μ_1, and an outer region with the properties k_2h, ϕ_2, μ_2. It is assumed that the active well is in the center of a cylindrically-shaped inner region and that the outer region is areally infinite. Mathematical solutions for drawdown and buildup in composite systems are given by several authors.[27,28,29] Figure 14 shows a typical pressure drawdown for a well located in the inner region. Initially, the drawdown is identical to that observed in an infinite system with the properties of the inner region. When

$$t_D = 0.25 = 2.64\text{x}10^{-4}k_1t/\phi_1\mu_1c_1a^2 \qquad (5)$$

the outer region begins to influence the data. After a transition period (whose duration depends on the size of the inner region, ϕch, and the ratio of the reservoir properties in the two regions) the outer region controls the pressure response. If the pressure response prior to this time is well-defined, the properties of the inner region can be calculated using methods developed for infinite systems. If the effects of both the inner and outer regions are observed in the data, there are several methods for calculating the radius of the inner region and the mobility of the outer region.[28,30,31]

For an observation well in the outer region, the pressure drawdown asymptotically approaches the solution for a homogeneous reservoir with the properties of the outer region.[29] Conventional semi-log analysis of the late-time data can be used to estimate the properties of the outer region.

For wells in the inner region, the above-mentioned methods of analysis are applicable only if the pressure transient data clearly reflect the presence of both regions. If k_1 is large and/or the inner region is small, the properties of the outer region quickly dominate the pressure response. In fact, the presence of the inner region may either go undetected or be mistaken for another form of reservoir heterogeneity. The following discussion pertains to just this situation, that is, when the existence of a composite reservoir is not recognized.

To further investigate this problem, the approximate solution for drawdown in a composite reservoir presented by Ramey[29] is examined. For an observation well in the inner region, the drawdown is approximated by

$$p_1(r,t) = p_i + \frac{q}{4\pi\lambda_1 h}\left\{Ei(-\varepsilon) - Ei\left(-\varepsilon\frac{a^2}{r^2}\right)\right.$$

$$\left. + \frac{\lambda_1}{\lambda_2}\, e^{-\varepsilon\left(\frac{a}{r}\right)^2}\left[1 - \frac{\eta_1}{\eta_2}\right] Ei\left(-\varepsilon\frac{a^2}{r^2}\frac{\eta_1}{\eta_2}\right)\right\} \qquad (6)$$

Assuming that $(\phi c)_1 = (\phi c)_2$, and that the logarithmic approximation of the Ei function is valid, equation 6 can be written as (in oilfield units)

$$\Delta p_1(r,t) = \frac{-162.6q}{\lambda_2 h}\left\{\frac{\lambda_2}{\lambda_1}\log\left(\frac{a}{r}\right)^2\right.$$

$$\left. + e^{-\left(\frac{948.0\,\phi c a^2}{\lambda_1 t}\left(1 - \frac{\lambda_1}{\lambda_2}\right)\right)\cdot\left(\log\left(\frac{\lambda_2 t}{\phi\mu a^2}\right) - 3.227\right)}\right\} \qquad (7)$$

For times greater than

$$t > \frac{948.0}{0.01} \frac{a^2 \phi c}{\lambda_1} \left| 1 - \frac{\lambda_1}{\lambda_2} \right| \quad (8)$$

the exponential term is within 1% of unity and equation 7 can be simplified to

$$\Delta p_1(r,t) = \frac{-162.6q}{\lambda_2 h} \left\{ \frac{\lambda_2}{\lambda_1} \log \left(\frac{a}{r}\right)^2 + \log t + \log \frac{\lambda_2}{\phi c a^2} - 3.227 \right\} \quad (9)$$

Equation 9 shows that the late-time data fall on a semi-log straight line whose slope is proportional to the properties of the outer region (assuming that equation 8 is satisfied and that the logarithmic approximation of Ei is valid). If this semi-log straight line is extrapolated until $\Delta p=0$, the intercept time(t_o) (see Figure 14) must satisfy the equation

$$\frac{\lambda_2}{\lambda_1} \log \left(\frac{a}{r}\right)^2 + \log t_o + \log \left(\frac{\lambda_2}{\phi c a^2}\right) - 3.227 = 0 \quad (10)$$

Rearranging, we see that

$$\phi ch = \left[5.929 \times 10^{-4} \frac{k_2 h / \mu_2}{r^2} t_o \right] \left(\frac{r}{a}\right)^{2\left(1 - \frac{\lambda_2}{\lambda_1}\right)} \quad (11)$$

This expression shows that ϕch is the product of two terms. The first is simply the expression for calculating ϕch in a homogeneous reservoir, henceforth referred to as the apparent storativity, ϕch_a. The second term in the equation indicates that the true ϕch of the reservoir differs from ϕch_a by a factor that depends on both the size of the inner region and the mobility contrast between the two regions. For example, in a composite reservoir with a higher mobility inner region, ϕch_a increases as the distance decreases between the pumped and observation wells.

This discussion shows that when the late-time semi-log straight line is used to calculate ϕch and the composite nature of the reservoir is not recognized, values of ϕch for wells in the inner region will be erroneous. Equation 11 shows that if r/a is small, even a small mobility contrast will result in a large discrepancy between the actual and calculated values of ϕch. In the following section it is shown that the systematic variations in ϕch_a can be used to calculate the size of the inner region and the mobility contrast between the two regions.

Analysis Technique

First, note that by taking the logarithm of both sides of equation 11, the equality can be expressed as

$$\log(\phi ch / \phi ch_a) = 2(1 - \lambda_2/\lambda_1)\log(r/a) \quad (12)$$

This implies that on a log-log plot of $(\phi ch/\phi ch_a)$ versus r, all of the data points from wells located in the inner region lie on a straight line with a slope of

$$b = 2(1 - \lambda_2/\lambda_1) \quad (13)$$

The mobility ratio between the inner and outer regions can be calculated by

$$\lambda_2/\lambda_1 = 1 - b/2 \quad (14)$$

In order to evaluate the radius of the inner region, it is necessary to have an estimate of the actual ϕch of the reservoir. This can be obtained from a well located in the outer region of the reservoir or an independent source (e.g., testing in nearby wells). In practice, one rarely knows a priori if a well is located in the inner or outer region. However, if more than one well, distant from the active well, yields the same or similar values of ϕch, it can be assumed that these wells are in the outer region. In general, it is better to have an independent check on ϕch from another source. Once ϕch is determined, the radius of the inner region is calculated by extrapolating the straight line drawn through the data points to the point where

$$\phi ch/\phi ch_a = 1 \quad \text{and} \quad a = r.$$

An alternative procedure is to construct a graph of $\log(\phi ch_a)$ versus $\log(r)$. The slope of the line through the data points is the negative of that given by equation 13 and λ_2/λ_1 is calculated from equation 14. The radius of the inner region is determined by extrapolating the straight line to the point where $\phi ch_a = \phi ch$ (and therefore, a = r).

Several additional points must be mentioned. First, the analysis method described above is only required when the pressure data unaffected by the outer region is of such short duration that it cannot be used for analysis of the properties of the inner region. In general, this only occurs if the inner region is very small (local heterogeneity) and/or the permeability of the inner region is very high. Otherwise, the response of the inner region will be clearly present and the data will be suitable for analysis using one of the existing methods. Second, the radius of the inner region can be estimated only if an accurate estimate of ϕch is available. However, the permeability contrast between the inner and outer regions can be calculated even if ϕch is not known. Third, by examining equation 13 we can place some constraints on the ratio $\phi ch/\phi ch_a$ that result from this type of model. Since λ_2/λ_1 must be positive, equation 13 requires that

$$b < 2 .$$

Also note that for

$$b > 0, \quad \lambda_1 > \lambda_2 ;$$

and for

$$b < 0, \quad \lambda_1 < \lambda_2 .$$

A final point is that this analysis procedure is based on the assumption that the inner region is cylindrically shaped and concentric around the pumped well. These assumptions may not always be appropriate for describing a geologic heterogeneity and therefore may limit the applicability of this approach. On the other hand, reservoir heterogeneities created by injection and production operations are often cylindrical and concentric around the active well. Therefore, this approach may be particularly useful for monitoring the progress of flooding operations and detecting production-induced changes in the reservoir.

Example

The values of ϕch_t calculated during the production phase of the interference test range from 1.1 to 4.8×10^{-3} ft/psi in the observation wells closest and furthest from CW-1, respectively. The average value of ϕch_t (considered to be representative of the actual value), calculated from the injection phase of the test, is 5×10^{-3} ft/psi. Figure 15 shows a log-log plot of $\phi ch/\phi ch_a$ versus the distance between the pumped and observation wells. A straight line with a slope of 1.73 can be drawn through the points. Using this slope and equation 14, we find that $\lambda_1/\lambda_2 = 7.4$. Since $\mu_1 = \mu_2$, $k_1/k_2 = 7.4$. The radius of the inner region is calculated by extrapolating the straight line through the data points to the point where $\phi ch = \phi ch_a$. As shown in the figure, a = 1600 ft.

In light of these unanticipated results, additional evidence for the existence of a high permeability region was sought. One such evidence comes from a graph of observation well drawdown vs. distance to the pumped well. For a homogeneous reservoir at semi-steady state, all of the data points should fall on a single straight line whose slope is inversely proportional to kh. Figure 16 shows the drawdown at each of the wells after 336 hours of pumping. As shown, the data points do not fall on a single straight line. Instead, with the exception of one data point, the data fall on two straight lines. The permeabilities of these two regions, calculated from the slopes of these lines, are 1.06×10^7 and 1.43×10^6 md-ft, respectively. The permeability calculated for the outer region agrees well with the average formation permeability calculated from the pressure transient analysis. Furthermore, the ratio of the inner to outer region permeability is approximately 7.4, the same value as that obtained from the above analysis. An inner region radius of 1100 ft is indicated from Figure 16, in comparison to the 1600 ft calculated above. The discrepancy between these two values may result from using an incorrect estimate of ϕch. Nevertheless, there is reasonable agreement between the two values.

Consideration of the geologic setting gives additional validity to this interpretation. A major range-front normal fault is known to transect the area. It was anticipated that the fault would manifest itself either as a constant pressure or no-flow linear boundary. Instead, the fault was essentially invisible to hydrologic testing. It is proposed here that in a limited area, the fault is not a single linear-fracture but a broad region coincident with the high permeability region detected from the interference test.

DISCUSSION

Two different models have been used to analyze the interference data presented here: a double-porosity model and a composite reservoir model. Conceptually, both models are appropriate from hydrogeologic considerations. Therefore, we must look to the data itself to determine the most convincing interpretation. The good matches between the double-porosity type-curves and the data, as well as the consistent values of kh calculated from them, suggest that this model is correct. However, values of ϕch_t, calculated using the double-porosity model, are anomalously high in some of the wells.

The apparent ambiguity between the two interpretations can be resolved by comparing the drawdown in a composite reservoir to that in a double-porosity reservoir. The solid line in Figure 17 shows the drawdown calculated for an observation well located in the inner region of a composite reservoir (properties are similar to those of the Klamath Falls reservoir). These drawdown data are analyzed using the previously described history-matching technique for double-porosity reservoirs. As shown in the triangles in Figure 17, the agreement between the two curves is excellent. Also note that the values of λ and ω are similar to the values of these parameters obtained from observation wells close to CW-1. The similarity between the drawdown curves for the different models shows that without additional information it may not be possible to determine which model is the correct one. However, since only the composite model can explain the variations in the apparent ϕch, this interpretation is the appropriate one for wells close to the pumped well.

Pressure buildup data from wells in the vicinity of the injection well behave like those of a double-porosity system. Greater consistency between the reservoir parameters obtained from the analyses of these data indicate that a double-porosity model more accurately fit the data near the injection well.

CONCLUSIONS

The results of the analysis can be summarized as follows. Interference data from the Klamath Falls geothermal reservoir are successfully analyzed using both a double-porosity and a composite reservoir model. Representative values of the formation parameters calculated from these models are

$$kh = 1.4 \times 10^6 \text{ md-ft}$$

$$\phi ch_t = 5 \times 10^{-3} \text{ ft/psi}$$

$$\lambda = 1 \times 10^{-7}$$

$$\omega = 1 \times 10^{-2}$$

The pumped well is located in a region that is approximately 7 1/2 times more permeable than the rest of the reservoir. This region is believed to coincide with a broad fault zone that transects the area.

Several other valuable conclusions can be drawn from this analysis.

1. Variations in ϕch may be indicative of lateral changes in the reservoir mobility. Systematic changes, in particular, can be interpreted to yield additional information about the reservoir properties.

2. A new graphical technique is available for analyzing data from composite systems. Based on variations in the apparent ϕch, the mobility contrast between the two regions and the radius of the inner region can be calculated.

3. Comparison of the results obtained from semi-log and type-curve analyses of double-porosity reservoirs show good agreement between the two techniques. In the majority of cases the calculated values of kh agree to within 10%, values of ϕch_t to within 35%, and the parameters λ and ω to within an order of magnitude. Given the extreme heterogeneity of this system, the agreement between these two techniques is very good. However, use of both techniques resulted in far greater confidence in the results of the analysis.

NOMENCLATURE

a	radius of the inner region of a composite reservoir	ft
B	formation volume factor	RB/stb
c	total compressibility $(c_w + c_r)$	1/psi
c_f	total fracture comp. $(c_w + c_f)$	1/psi
c_m	total matrix comp. $(c_w + c_m)$	1/psi
h	reservoir thickness	ft
k	absolute permeability	md
p	pressure	psi
p_D	dimensionless pressure $(2\pi kh\Delta p/qB\mu)$	-
r	radial distance between the production and observation wells	ft
r_D	dimensionless radius (r/r_w)	-
q	volumetric flowrate	stb/D
t	time	hours
t_D	dimensionless time	-
t_i	intersection of the first semi-log straight line with $\Delta p = 0$	hours
t_o	intersection of the second semi-log straight line with $\Delta p = 0$	hours
λ	$\alpha r_w^2(k_m/k_f)$	-
λ_1	mobility of the inner region	md/cp
λ_2	mobility of the outer region	md/cp
ϕ	porosity	-
ϕch	storativity	ft/psi
ϕch_a	apparent storativity	ft/psi
ϕch_t	total storativity $(\phi_f c_f + \phi_m c_m)h$	ft/psi
μ	fluid viscosity	cp
α	geometric shape factor	m^2
ε	$r^2/4\eta_1 t$	-
η	diffusivity $(k/\phi\mu c)$	m^2/s
ω	$\phi_f c_f/(\phi_f c_f + \phi_m c_m)$	-

Subscripts
1 Inner region
2 Outer region

ACKNOWLEDGEMENTS

The invaluable efforts of Ray Solbau, who made collection of these data possible, are gratefully acknowledged. Thanks are also due to Mary Bodvarsson who helped in the preparation of this manuscript. This work was supported by the Assistant Secretary for Conservation and Renewable Energy, Office of Renewable Technology, Division of Geothermal and Hydropower Technologies of the U.S. Department of Energy under contract no. DE-AC03-76SF00098.

REFERENCES

1. Bixel, H. C., Larkin, B. K., and van Poollen, H. K.: "Effect of Linear Disconitinuities on Pressure Build-up and Drawdown Behavior," JPT (Aug. 1963), p. 885-895.

2. Ramey, H. J., Jr.: "Interference Analysis for Anisotropic Formations - A Case History," JPT (Oct. 1972), p. 1290-1298.

3. Hurst, W.: "Interference Between Oil Fields," Trans. AIME (1960), p. 175-192.

4. Woods, E.G.: "Pulse Test Response of a Two-Zone Reservoir," SPEJ (Sept. 1970), p. 245-255.

5. Kazemi, H., Seth, M.S., and Thomas, G. W.: "The Interpretation of Interference Tests in Naturally Fractured Reservoirs With Uniform Fracture Distribution," SPEJ (Dec. 1969), p. 463-472.

6. Earlougher, R. C.: Advances in Well Test Analysis, Monograph Series, Society of Petroleum Engineers of AIME, Dallas (1977).

7. Sammel, E. A.: Hydrogeologic Appraisal of the Klamath Falls Geothermal Area, Oregon, U.S. Geological Survey Professional Paper 1044-G (1980).

8. Sammel, E. A.: Analysis and Interpretation of Data Obtained in Tests of the Geothermal Aquifer at Klamath Falls, Oregon, U.S. Geological Survey Water Resources Investigations Report 84-4216, (1984).

9. Culver, G. G., Lund, J. W., and Svanevik, L. S.: Klamath Falls Hot Water Well Study, Lawrence Livermore Laboratory Report, UCRL-13614, (1974).

10. Peterson, N. V., and McIntyre, J. R.: The Reconnaissance Geology and Mineral Resources of Eastern Klamath County and Western Lake County, Oregon, Oregon Dept. of Geology and Minerals Industrial Bull., (1970).

11. Meyers, J. D., and Newcomb, R. C.: Geology and Ground-Water Resources of the Swan Lake-Yonna Valleys Area, Klamath County, Oregon, U.S. Dept. of the Interior, (1952).

12. Benson, S. M., and others: Data From Pumping and Injection Tests and Chemical Sampling in the Geothermal Aquifer at Klamath Falls, Oregon, U.S. Geological Survey Open-File Report 84-146, (1984).

13. Benson, S. M., Goranson C. B., and Schroeder, R. C.: Evaluation of City Well 1, Klamath Falls, Oregon, Lawrence Berkeley Laboratory Report, LBL-10848, (1980).

14. Lund, J. W.: Geothermal Hydrology and Geothermal Geochemistry of the Klamath Falls, Oregon Urban Area, final report to the U.S. Geological Survey, Grant N. 14-08-0001-G-29, (1978).

15. Bodvarsson, M. G., and Benson, S. M.: Well Test Data From Geothermal Reservoirs, Lawrence Berkeley Laboratory Report, LBL-13295, (1982).

16. Deruyck, B. G., Bourdet, D. P., Da Prat, G., and Ramey, H. J., Jr,: "Interpretation of Interference Tests in Double-Porosity Reservoirs - Theory and Field Example," presented at the 57th Annual Meeting of the Society of Petroluem Engineers of the AIME., New Orleans, LA.,(1982).

17. Solbau, R. D., Goranson, C. B., and Benson, S. M.: Recently Developed Instrumentation for Low-to-Moderate Temperature Geothermal Reservoirs, Lawrence Berkeley Laboratory Report, LBL-13260, (1981).

18. Benson, S. M.: "Interpretation of Interference Data From the Klamath Falls Geothermal Resource, Oregon," GEO-HEAT CENTER Quarterly Bulletin, v. 8, no. 2, Oregon Institute of Technology, Klamath Falls, Oregon.

19. Warren, J. E., and Root, P. J.: "The Behavior of Naturally Fractured Reservoirs," SPEJ (Sept. 1963), p. 245-255.

20. Serra, K. V., Reynolds, A. C., and Raghavan, R.: "New Pressure Transient Analysis Methods for Naturally Fractured Reservoirs," presented at the 1982 California Regional Meeting of the Society of Petroleum Engineers, San Francisco, California, SPE-10780, (1982).

21. Odeh, A. S.: "Unsteady-State Behavior of Naturally Fractured Reservoirs," SPEJ (March 1965), p. 60-64.

22. Lai, C. H., Bodvarsson, G. S., and Witherspoon, P. A.: "A New Model for Well-Test Data Analysis in Naturally Fractured Reservoirs," presented at the 1983 California Regional Meeting of the Society of Petroleum Engineers, Ventura, California, SPE-11688, (1983).

23. Streltsova, T. D.: "Well Pressure Behavior of a Naturally Fractured Reservoir," presented at the 1982 California Regional Meeting of the Society of Petroleum Engineers, San Fransisco, California, SPE-10782, (1982).

24. Barenblatt, G. I., and Zheltov, I. P.: "On the Basic Flow Equations of Homogeneous Liquids in Fissured Rocks," Dokl. Akad. Nauk SSSR (1960), 132, N3, p. 545-548.

25. Moench, A. F.: "Well Test Data Analysis in Naturally Fissured Geothermal Reservoirs With Fracture Skin," in proceedings of the Ninth Workshop on Geothermal Reservoir Engineering, Stanford University, (Dec. 1983), p. 175-180.

26. O'Brien, M. T., and Benson, S. M.: "Reservoir Evaluation of Klamath Falls, Oregon," in 1980 Annual Report of the Earth Sciences Division, Lawrence Berkeley Laboratory Report, LBL-12100 (1980).

27. Larkin, B. K.: "Solutions to the Diffusion Equation for a Region Bounded by a Circular Discontinuity," SPEJ (June 1963), p. 113-115.

28. Odeh, A. S.: "Flow Test Analysis for a Well With Radial Discontinuity," JPT (Feb. 1969), p. 207-210.

29. Ramey, H. J., Jr.: "Approximate Solutions for Unsteady Liquid Flow in Composite Reservoirs," Journal of Canadian Petroleum Technology (March, 1970), p. 32-37.

30. Merrill, L. S., Kazemi, H., and Gogarty, W.: "Pressure Falloff Analysis in Reservoirs with Fluid Banks," JPT (July, 1974), p. 809-818.

31. Bixel, H. C., and van Poollen, H. K.: "Pressure Drawdown and Build-Up in the Presence of Radial Discontinuities," SPEJ (Sept. 1967), p. 310-309.

Well	Depth (ft)	Elevation (ft)	Distance CW-1 (ft)	Distance to Inj. Well (ft)
Carroll	303	4220	540	3200
Parks	765	4189	710	3460
Assembly	363	4163	1285	3460
Medo-Bel	765	4115	2740	630
Head	250	n.a.	1050	2100
S&M	900	4107	2100	750
Page	465	4120	2200	850
Rogers	329	4190	410	2650
Steamer	250(?)	4195	122	2850
CW-1(1)	900	4200	-0-	2750
C. Museum(2)	1235	4115	2750	-0-

(1) Produces from 195-240 ft
(2) Produces from 470-520 ft and 1020-1080 ft

Table 1. Well depths, production intervals and distances to CW-1 and the County Museum wells.

Well	kh (md-ft)	ϕ ch (ft/psi)	ω	λ	Active well
Page	1.7×10^{6} (1.7×10^{6})	5.7×10^{-3} (4.8×10^{-3})	0.3 (0.1)	1.9×10^{-7} (6.0×10^{-7})	CW-1
Assembly	1.7×10^{6} (1.5×10^{6})	5.1×10^{-3} (6.9×10^{-3})	0.01 (0.02)	2.7×10^{-7} (1.0×10^{-7})	CW-1
Head	1.4×10^{6} (1.4×10^{6})	9.5×10^{-3} (1.1×10^{-2})	0.01 (0.02)	4.1×10^{-7} (2.2×10^{-7})	CW-1
Parks	1.7×10^{6} (1.9×10^{6})	3.0×10^{-2} (2.2×10^{-2})	0.01 (0.04)	1.7×10^{-6} (1.3×10^{-6})	CW-1
Carroll	1.5×10^{6} (1.5×10^{6})	2.6×10^{-2} (2.7×10^{-2})	0.015 (0.01)	1.1×10^{-6} (7.5×10^{-7})	CW-1
Rogers	1.4×10^{6} (1.3×10^{6})	6.6×10^{-2} (5.9×10^{-2})	0.03 (0.01)	4.0×10^{-6} (2.0×10^{-6})	CW-1
Steamer	1.3×10^{6} (1.1×10^{6})	0.79 (1.1)	0.01 (0.001)	1.5×10^{-5} (1.5×10^{-5})	CW-1
Carroll	1.3×10^{6} (1.2×10^{6})	2.3×10^{-3} (2.3×10^{-3})	0.3 (0.1)	2.2×10^{-7} (1.5×10^{-6})	INJ
Steamer	1.4×10^{6} (1.4×10^{6})	3.2×10^{-3} (2.6×10^{-3})	n.a.	n.a.	INJ
Head	1.2×10^{6} (1.4×10^{6})	6.1×10^{-3} (4.6×10^{-3})	0.3 (0.3)	5.1×10^{-7} (5.0×10^{-6})	INJ
Page	1.4×10^{6} (1.3×10^{6})	7.3×10^{-3} (7.8×10^{-3})	0.06 (0.02)	2.4×10^{-7} (3.0×10^{-7})	INJ
S&M	1.3×10^{6} (1.0×10^{6})	6.0×10^{-3} (7.9×10^{-3})	0.06 (0.003)	1.8×10^{-7} (3.0×10^{-7})	INJ
Medo Bel	1.1×10^{6} (1.1×10^{6})	1.1×10^{-3} (2.8×10^{-3})	0.15 (0.04)	2.7×10^{-8} (9.0×10^{-8})	INJ

Table 2. Summary of type-curve and semi-log analyses (semi-log results shown in parenthesis).

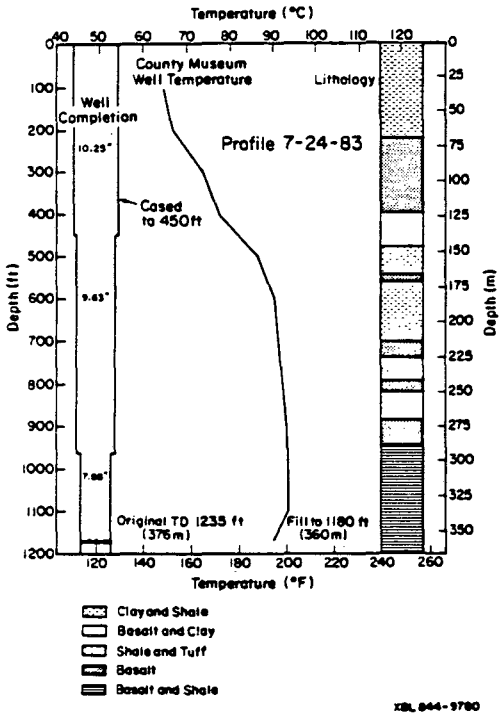

Figure 1. Well lithology, completion, and temperature profile for the County Museum Well.

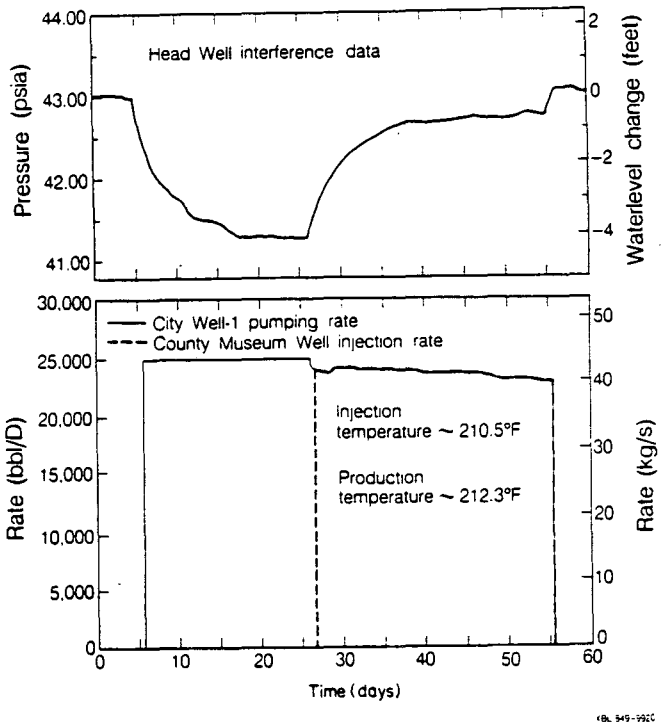

Figure 2. Pumping, injection, and observation well data from the interference test.

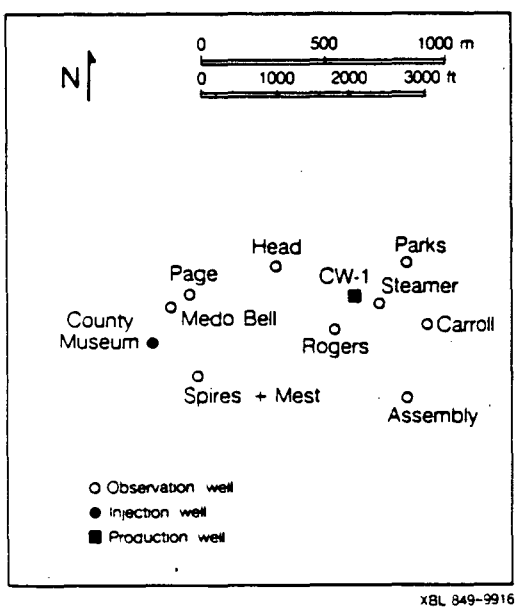

Figure 3. Pumping, injection and observation well locations.

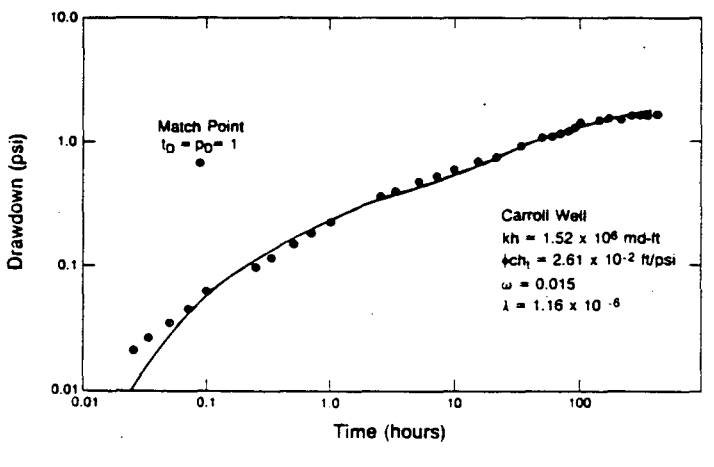

Figure 4. Log-log plot and double-porosity type-curve match for the Carroll well drawdown data.

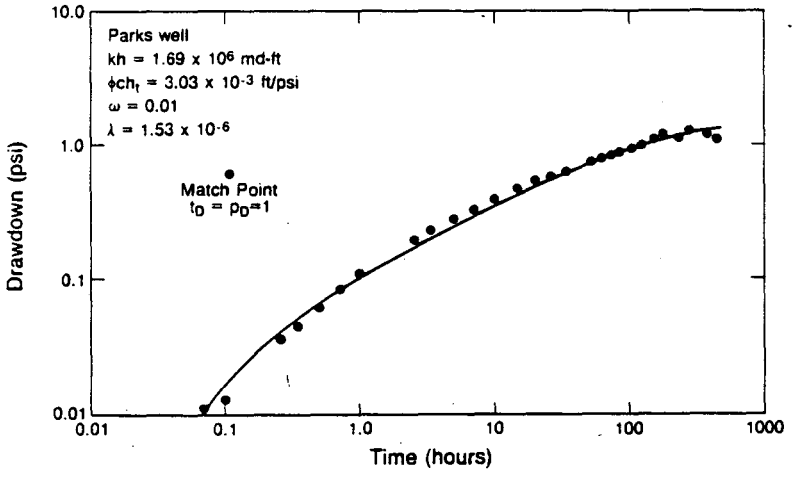

Figure 5. Log-log plot and double-porosity type-curve match for the Parks well drawdown data.

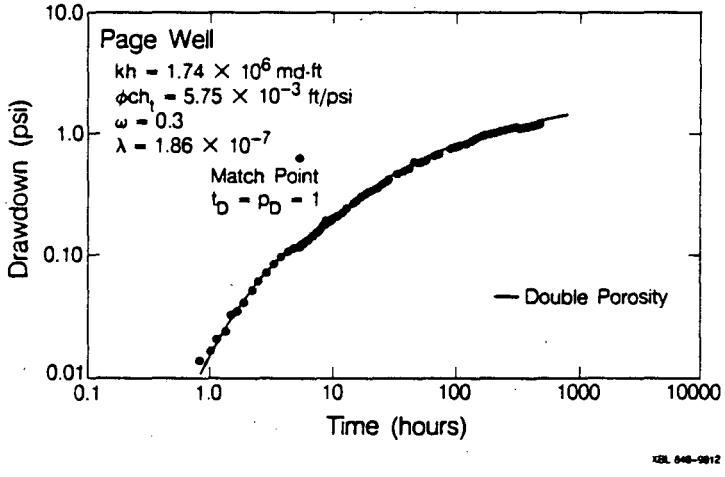

Figure 6. Log-log plot and double-porosity type-curve match for the Page well drawdown data.

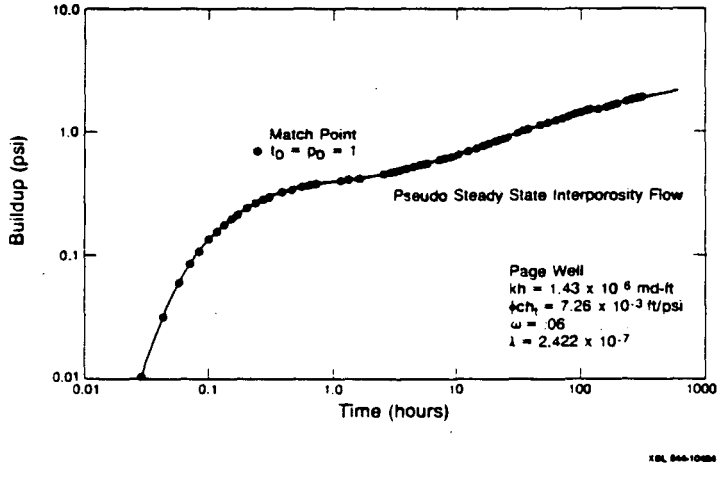

Figure 7. Log-log plot and double-porosity type-curve match for the Page well buildup data.

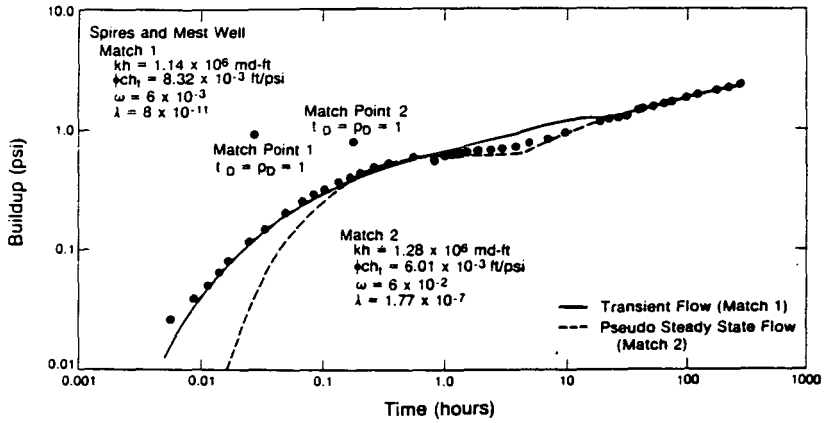

Figure 8. Log-log plot and double-porosity type-curve matches for the Spires & Mest well buildup data.

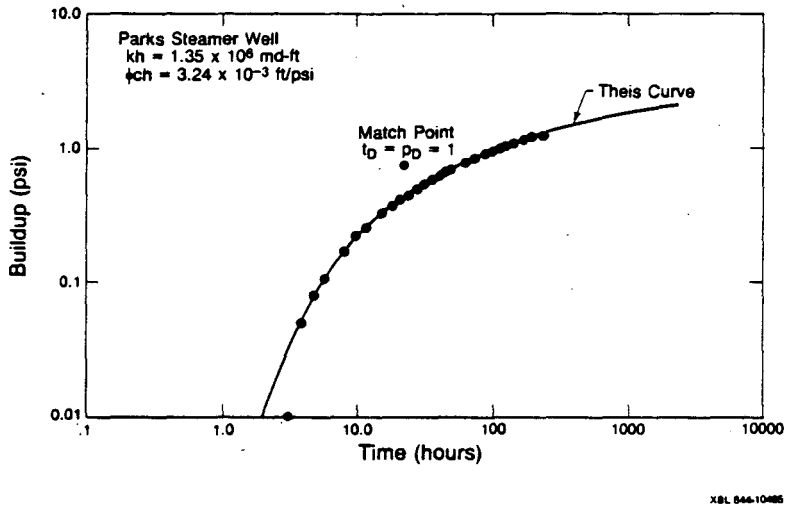

Figure 9. Log-log plot and Theis curve match for the Parks Steamer well buildup data.

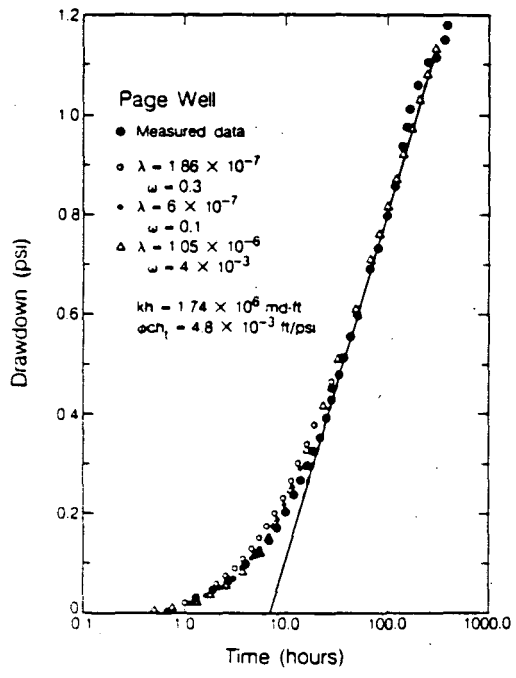

Figure 10. Semi-log plot and double-porosity analysis of the Page well drawdown data.

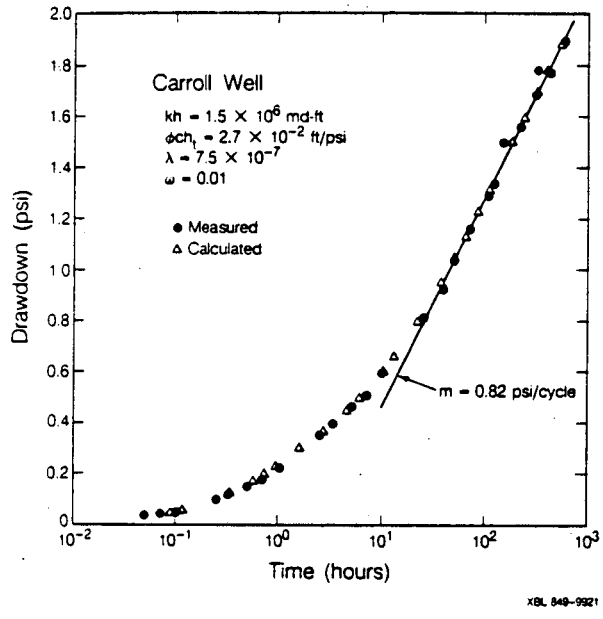

Figure 11. Semi-log plot and double-porosity history-match for the Carroll well drawdown data.

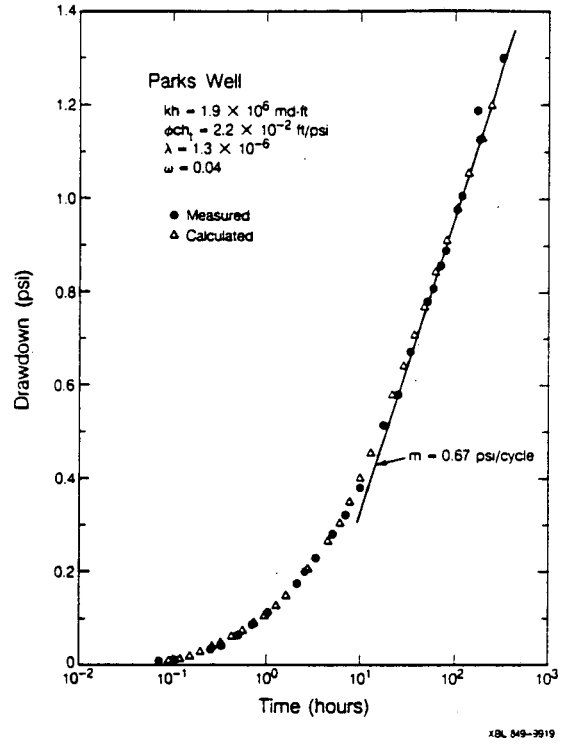

Figure 12. Semi-log plot and double-porosity history-match for the Parks well buildup data.

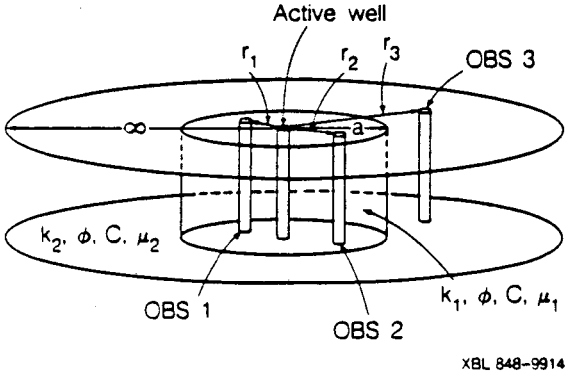

Figure 13. Schematic of a composite reservoir.

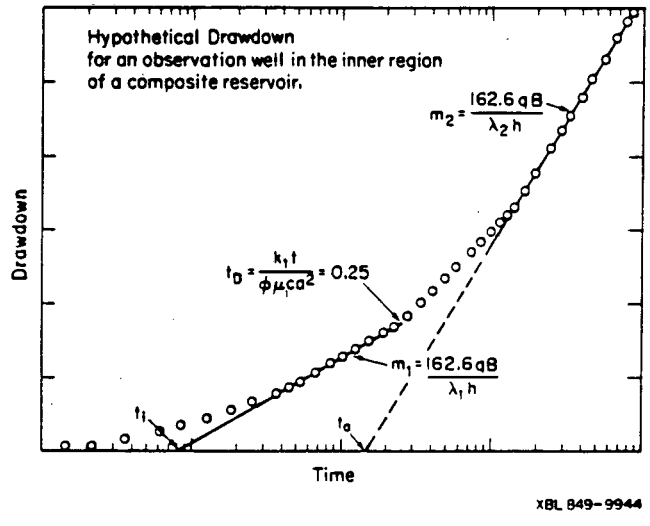

Figure 14. Semi-log plot of the hypothetical drawdown for an observation well located in the inner-region of a composite reservoir.

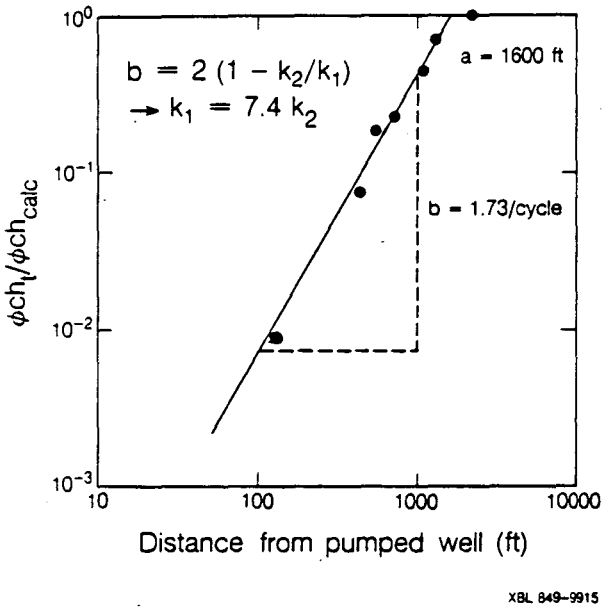

Figure 15. Composite reservoir analysis for the Klamath Falls interference data.

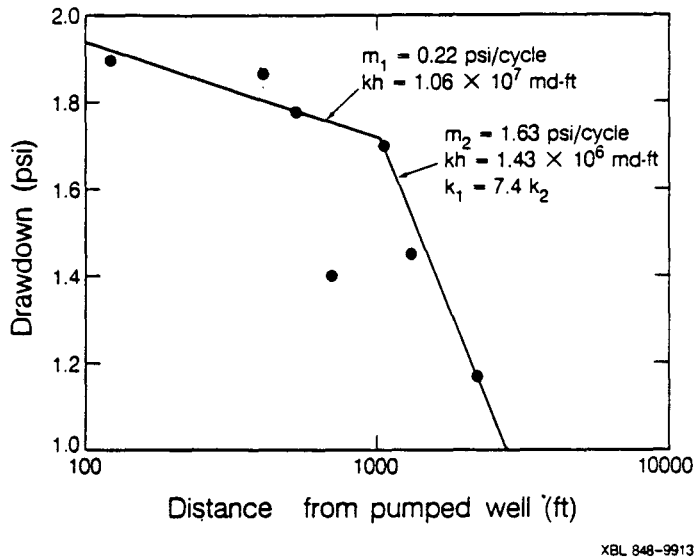

Figure 16. Pressure drawdown (at 336 hours) versus distance to the pumping well.

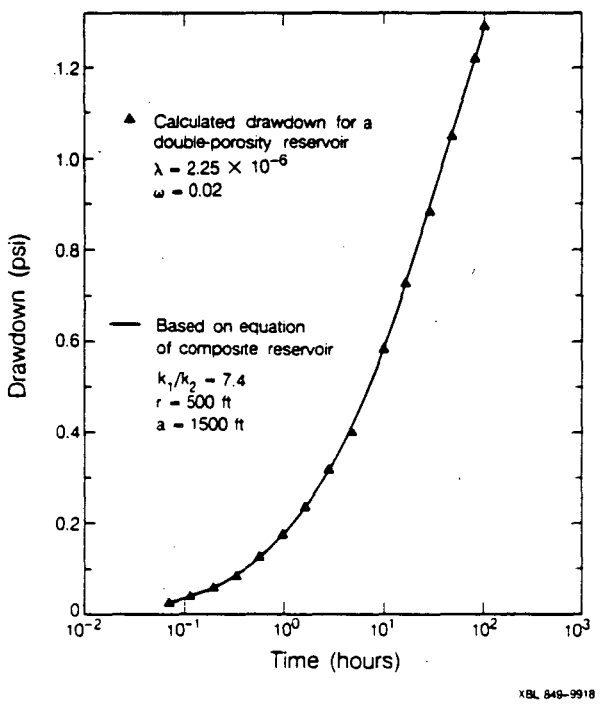

Figure 17. Match between the drawdowns in a hypothetical composite reservoir and a double-porosity reservoir.

TECHNICAL INFORMATION DEPARTMENT
LAWRENCE BERKELEY LABORATORY
UNIVERSITY OF CALIFORNIA
BERKELEY, CALIFORNIA 94720